Resistivity Measurements on Germanium for Transistors*

L. B. VALDES†, MEMBER, IRE

Summary—This paper discusses a laboratory method which has been found very useful for measuring the resistivity of the semiconductor germanium. The method consists of placing four probes that make contact along a line on the surface of the material. Current is passed through the outer pair of probes and the floating potential is measured across the inner pair. There are seven cases considered, the probes on a semi-infinite volume of semiconductor material and the probes near six different types of boundaries. Formulas and curves needed to compute resistivity are given for each case.

INTRODUCTION

THE PROPERTIES of the bulk material used for the fabrication of transistors and other semiconductor devices are essential in determining the characteristics of the completed devices. Resistivity and lifetime[1] (of minority carriers) measurements are generally made on germanium crystals to determine their suitability. The resistivity, in particular, must be measured accurately since its value is critical in many devices. The value of some transistor parameters, like the equivalent base resistance,[2] are at least linearly related to the resistivity.

Many conventional methods for measuring resistivity are unsatisfactory for germanium because it is a semiconductor and metal-semiconductor contacts are usually rectifying in nature. Also there is generally minority carrier injection by one of the current carrying contacts. An excess concentration of minority carriers will affects the potential of other contacts[3] and modulate the resistance of the material.[4]

The method described here overcomes the difficulties mentioned above and also offers several other advantages. It permits measurement of resistivity in samples having a wide variety of shapes, including the resistivity of small volumes within bigger pieces of germanium. In this manner the resistivity on both sides of a *p-n* junction can be determined with good accuracy before the material is cut into bars for making devices. This method of measurement is also applicable to silicon and other semiconductor materials.

The basic model for all these measurements is indicated in Fig. 1. Four sharp probes are placed on a flat

surface of the material to be measured, current is passed through the two outer electrodes, and the floating potential is measured across the inner pair. If the flat surface on which the probes rest is adequately large and the crystal is big the germanium may be considered to be a semi-infinite volume. To prevent minority carrier injection and make good contact, the surface on which the probes rest may be mechanically lapped.
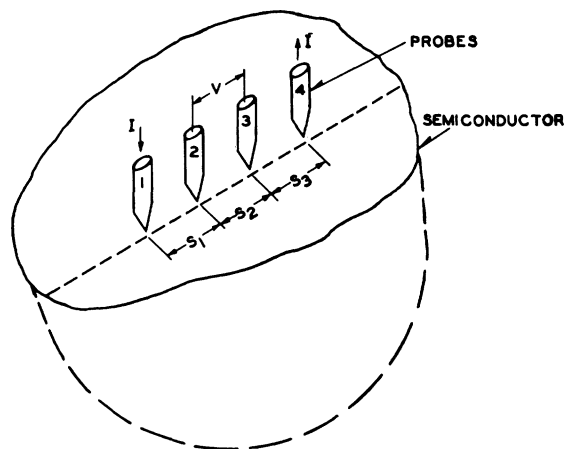

Fig. 1—Model for the four probe resistivity measurements.

The experimental circuit used for measurement is illustrated schematically in Fig. 2. A nominal value of probe spacing which has been found satisfactory is an equal distance of 0.050 inch between adjacent probes. This permit measurement with reasonable currents of *n*- or *p*-type germanium from 0.001 to 50 ohm-cm.

The simple case of four probes on a semi-infinite volume of germanium, which has been solved previously by W. Shockley and others,[5] is repeated here for complete-
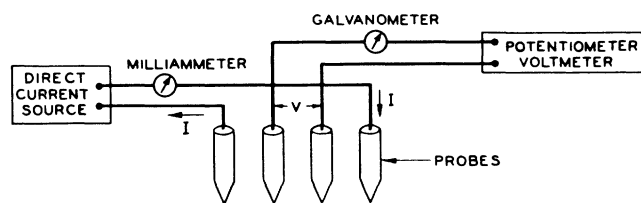

Fig. 2—Circuit used for resistivity measurements.

[1] L. B. Valdes, "Measurement of minority carrier lifetime in germanium," PROC. I.R.E., vol. 40, pp. 1420–1423; November, 1952.
[2] L. B. Valdes, "Effect of electrode spacing on the equivalent base resistance of point-contact transistors," PROC. I.R.E., vol. 40, pp. 1429–1434; November, 1952.
[3] J. Bardeen, "Theory of relation between hole concentration and characteristics of germanium point contacts," *Bell Sys. Tech. Jour.*, vol. 29, pp. 469–495; October, 1950.
[4] W. Schockley, G. L. Pearson, J. R. Haynes, "Hole injection in germanium-quantitative studies and filamentary transistors," *Bell Sys. Tech. Jour.*, vol. 28, pp. 344–366; July, 1949.

[5] The author has been informed that this method is the same as used in earth resistivity measurements. Some of the more pertinent references in that field are:
(a) F. Ollendorff, "Erdstrome," Julius Springer, Berlin, Germany; 1928.
(b) J. Riordan and E. D. Sunde, "Mutual impedance of grounded wires for horizontally stratified two-layer earth," *Bell Sys. Tech. Jour.*, vol. 12, pp. 162–177; April, 1933.
(c) E. D. Sunde, "Earth Conduction Effects in Transmission Systems," D. Van Nostrand Co., Inc., New York, N. Y., pp. 47–51; 1949.

ness. Three cases of plane boundaries parallel and perpendicular to the surface where the measurement is made are solved for both conducting and nonconducting boundaries.

In order to use this four probe method in germanium crystals or slices it is necessary to assume that:

1. The resistivity of the material is uniform in the area of measurement.

2. If there is minority carrier injection into the semiconductor by the current-carrying electrodes most of the carriers recombine near the electrodes so that their effect on the conductivity is negligible. (This means that the measurements should be made on surfaces which have a high recombination rate, such as mechanically lapped surfaces.)

3. The surface on which the probes rest is flat with no surface leakage.

4. The four probes used for resistivity measurements contact the surface at points that lie in a straight line.

5. The diameter of the contact between the metallic probes and the semiconductor should be small compared to the distance between probes.

6. The boundary between the current-carrying electrodes and the bulk material is hemispherical and small in diameter.

7. The surfaces of the germanium crystal may be either conducting or nonconducting.

(a) A conducting boundary is one on which a material of much lower resistivity than germanium (such as copper) has been plated.

(b) A nonconducting boundary is produced when the surface of the crystal is in contact with an insulator.

The derivation of equations is considered in the appendix. Only the final results for each of the cases are presented here.

Case 1. Resistivity Measurements on a Large Sample

The model for a semi-infinite volume of material is in Fig. 1. This is approximated by a large sample, such as a crystal or part of it. The resistivity is computed as

$$\rho = \frac{V}{I} \frac{2\pi}{\left(\dfrac{1}{s_1} + \dfrac{1}{s_3} - \dfrac{1}{s_1 + s_2} - \dfrac{1}{s_2 + s_3} \right)} \qquad (1)$$

where

$V =$ floating potential difference between the inner probes, volts

$I =$ current through the outer pair of probes, amps

$s_1, s_2, s_3 =$ point spacing, in cm

$\rho =$ resistivity in ohm-cm.

When $s_1 = s_2 = s_3 = s$ (1) simplifies to:

$$\rho = \frac{V}{I} 2\pi s. \qquad (2)$$

Case 2. Resistivity Probes Perpendicular to a Nonconducting Boundary

The model is in Fig. 3. The boundary is perpendicular to the surface where the measurement is made and is also nonconducting. The probes are perpendicular to the boundary. The resistivity may be calculated from

$$\rho = \rho_0 F_2 \left(\frac{l}{s} \right) \qquad (3)$$

where ρ_0 is computed from (2) and $F_2(l/s)$ is plotted in Fig. 4. The distance l between the nearest probe and the boundary and the point spacing s are defined in Fig. 3.
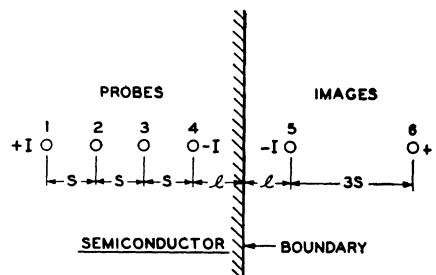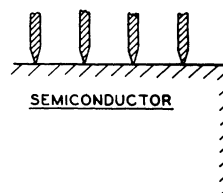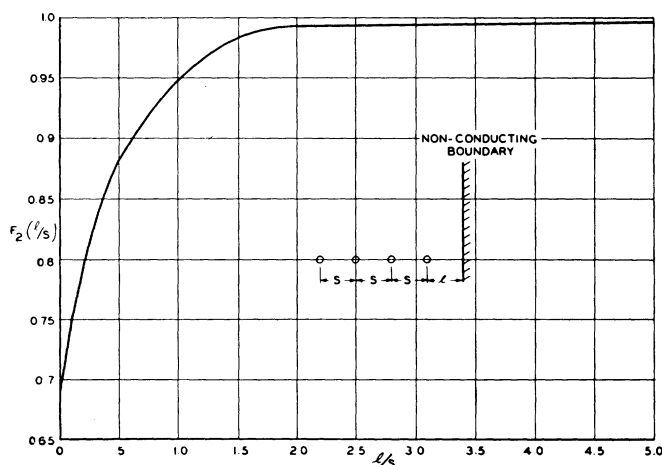

Fig. 3—Resistivity probes perpendicular to a boundary.

Fig. 4—Correction factor for probes perpendicular to a nonconducting boundary.

The resistivity ρ_0 may be computed from (1) if the point spacings differ but are approximately equal to within 5 per cent.
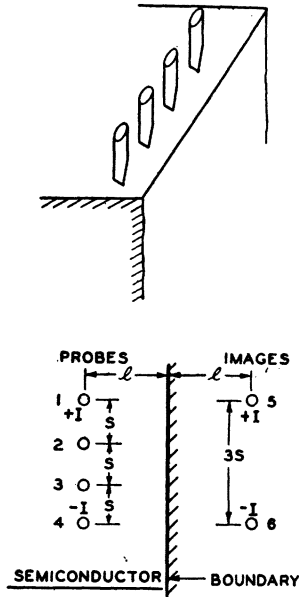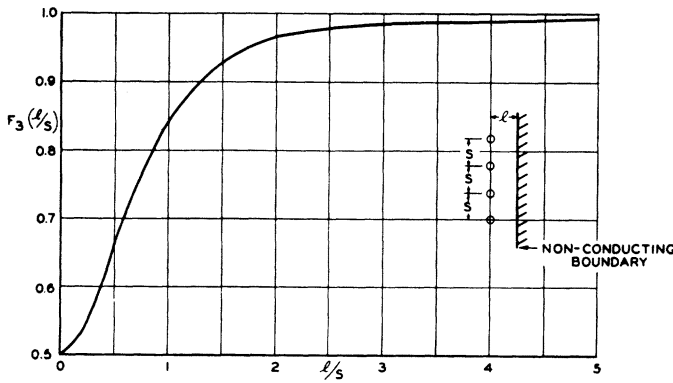
Fig. 5—Resistivity probes parallel to a boundary.

Fig. 6—Correction factor for probes parallel to a
nonconducting boundary.

Fig. 7—Correction factor for probes perpendicular to a
conducting boundary.

Fig. 8—Correction factor for probes parallel to a
conducting boundary.

Case 3. Resistivity Probes Parallel to a Nonconducting Boundary

The model is given in Fig. 5. It is the same as for Case 2 except that the probes are parallel to the boundary. The resistivity is

$$\rho = \rho_0 F_3\left(\frac{l}{s}\right) \tag{4}$$

where ρ_0 is defined as before and $F_3(l/s)$ is plotted in Fig. 6.

Case 4. Resistivity Probes Perpendicular to a Conducting Boundary

This differs from Case 2 only in that the boundary is a good conductor of electricity. Such boundary might be obtained by plating that face of the semiconductor with a metal such as copper. The model of Fig. 3 essentially describes the geometry of this case. The resistivity is
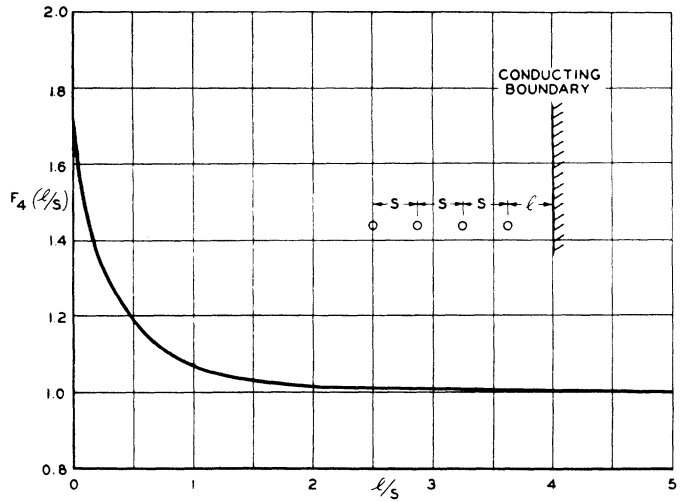
$$\rho = \rho_0 F_4\left(\frac{l}{s}\right) \tag{5}$$
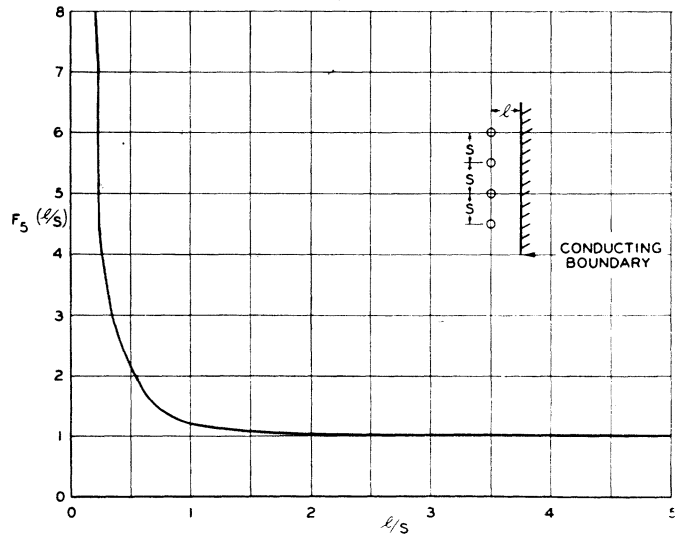
where ρ_0 is defined as before and $F_4(l/s)$ is plotted in Fig. 7.

Case 5. Resistivity Probes Parallel to a Conducting Boundary

The same model of Fig. 5 is applicable except for the conducting type of boundary. The resistivity is

$$\rho = \rho_0 F_5\left(\frac{l}{s}\right) \tag{6}$$

and $F_5(l/s)$ is plotted in Fig. 8.

Case 6. Resistivity Measurements on a Thin Slice-Conducting Bottom Surface

Fig. 9 shows the resistivity probes on a die of material. If the side boundaries are adequately far from the probes the die may be considered to be identical to a slice. For this case of a slice of thickness w and with a conducting bottom surface the resistivity is computed
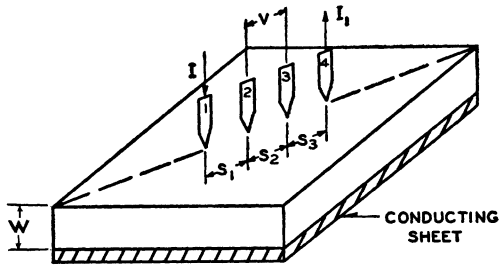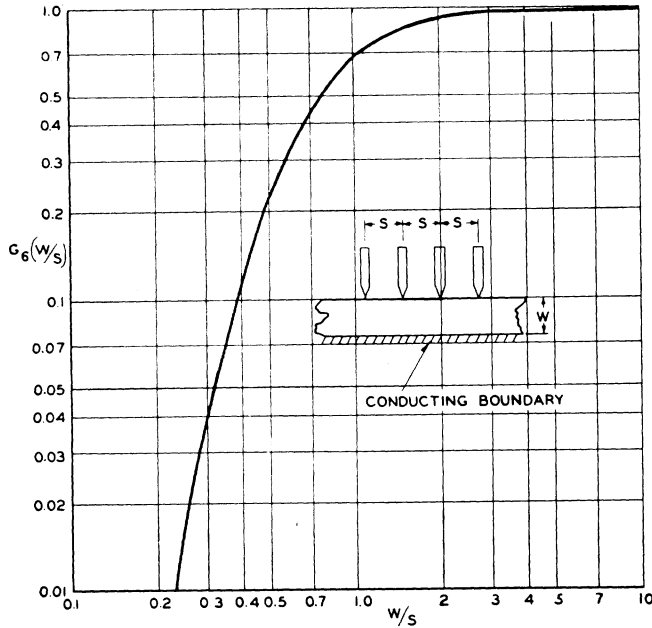
Fig. 9—Resistivity measurements on a thin slice.

Fig. 10—Correction divisor for probes on a thin slice with a conducting bottom surface.
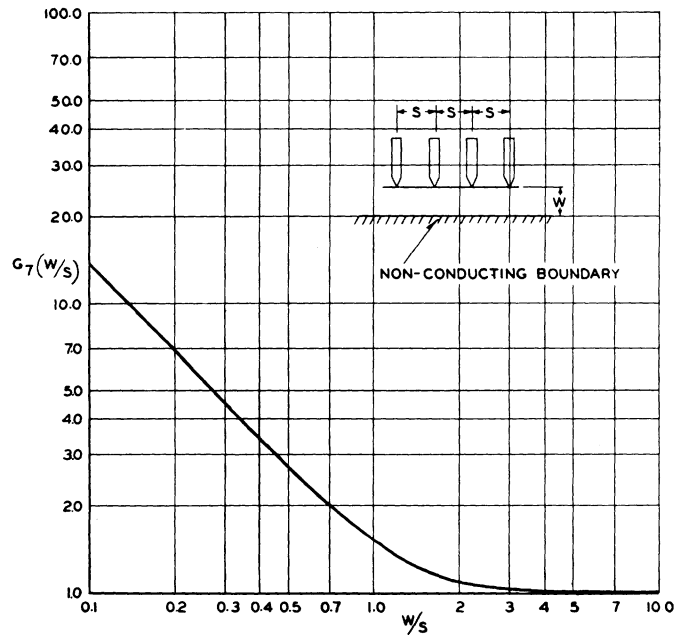

Fig. 11—Correction divisor for probes on a thin slice with a nonconducting bottom surface.

Fig. 12—Experimental check for resistivity probes perpendicular to a nonconducting boundary.

by means of the divisor $G_6(w/s)$ of Fig. 10 as:

$$\rho = \frac{\rho_0}{G_6\left(\dfrac{w}{s}\right)}. \qquad (7)$$

This method is not recommended for w/s very small.

Case 7. Resistivity Measurements on a Thin Slice-Non-conducting Bottom Surface

For the case of a nonconducting bottom on a slice like that of Case 6, the resistivity is computed from

$$\rho = \frac{\rho_0}{G_7\left(\dfrac{w}{s}\right)}. \qquad (8)$$

The function $G_7(w/s)$ is shown in Fig. 11 and ρ_0 is obtained as defined previously from either (1) or (2).

Results

An experimental check has been obtained from Cases 2 and 3. These are the two cases where a nonconducting side boundary was considered. Case 2 is for the probes perpendicular to the boundary and the agreement be-

tween theory and experiment is shown in Fig. 12. Case 3 assumes the probes to be parallel to the boundary and the results are in Fig. 13. Both of these curves show the uncorrected value of resistivity ρ_0 calculated from (1) at different ratios l/s. These values are shown as circled dots. The corrected experimental values ρ obtained by means of (3) and (4) and of Figs. 4 and 6 are shown by crosses. Using the mean value of ρ smooth curves have been drawn to indicate the way that ρ_0 should vary if the material is of constant resistivity and there is almost perfect agreement between theory and experiment. All experimental values shown on these curves represent the average of four readings taken with probes spaced about 0.050 inch apart.

The effect of the current flowing through the outer probes on the measured resistivity has been investigated by one set of readings taken on a 6.3 ohm-cm sample. The results are plotted in Fig. 14. The 37 per cent reduction in resistivity at 100 ma is believed to be

due primarily to heating of the sample, since its temperature was at least 30° C above ambient with this high current. All resistivity measurements are ordinarily done with 1 ma through the probes.
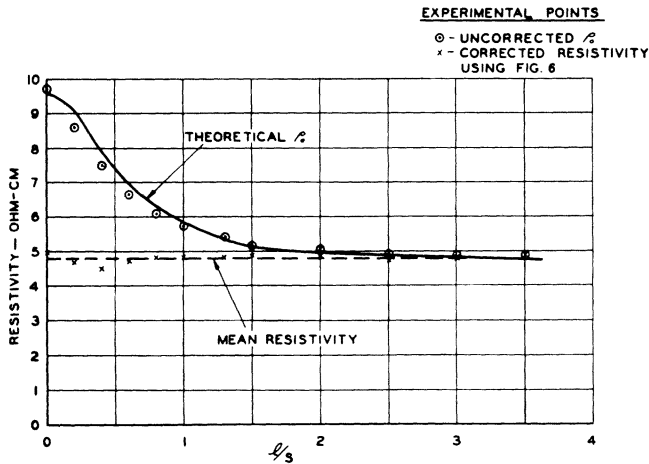

Fig. 13—Experimental check for resistivity probes parallel to a nonconducting boundary.

APPENDIX

DEVIATION OF FORMULAS

In this appendix are derived the formulas used in this paper for the computation of resistivity. This discussion will be limited to the four point method.

To treat the various models several general assumptions have been made. These were stated in the text and are not repeated here.
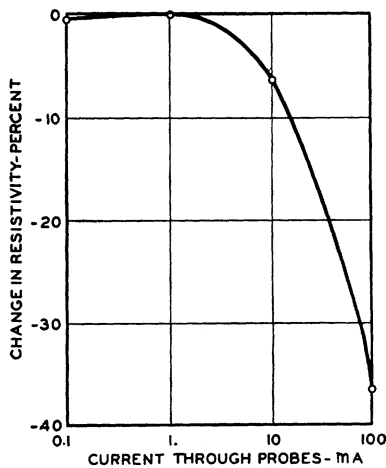

Fig. 14—Effect of current on measured resistivity.

Seven different geometries will be analyzed here. These are: 1. the four point probes on a semi-infinite volume of germanium; 2. the probes near a nonconducting boundary and perpendicular to it; 3. the probes parallel to a nonconducting boundary; 4. the probes perpendicular to a conducting boundary; 5. the probes parallel to a conducting boundary; 6. the probes on a thin slice where the bottom surface is conducting; and 7. the probes on a slice with a nonconducting bottom surface.

Case 1. Resistivity Measurements on a Large Sample

One added boundary condition is required to treat this case, namely, that the probes are far from any of the other surfaces of the sample and the sample can thus be considered a semi-infinite volume of uniform resistivity material. Fig. 1 shows the geometry of this case. Four probes are spaced s_1, s_2, and s_3 apart. Current I is passed through the outer probes (1 and 4) and the floating potential V is measured across the inner pair of probes 2 and 3.

The floating potential V_f a distance r from an electrode carrying a current I in a material of resistivity ρ is given by[6]

$$V_f = \frac{\rho I}{2\pi r}. \tag{9}$$

In the model shown in Fig. 1 there are two current-carrying electrodes, numbered 1 and 4, and the floating potential V_f, at any point in the semiconductor is the difference between the potential induced by each of the electrodes, since they carry currents of equal magnitude but in opposite directions. Thus:

$$V_f = \frac{\rho I}{2\pi}\left(\frac{1}{r_1} - \frac{1}{r_4}\right) \tag{10}$$

where:

r_1 = distance from probe number 1.
r_4 = distance from probe number 4.

The floating potentials at probe (2) V_{f_2} and at probe (3) V_{f_3} can be calculated from (10) by substituting the proper distances as follows:

$$V_{f_2} = \frac{\rho I}{2\pi}\left(\frac{1}{s_1} - \frac{1}{s_2 + s_3}\right) \tag{11}$$

$$V_{f_3} = \frac{\rho I}{2\pi}\left(\frac{1}{s_1 + s_2} - \frac{1}{s_3}\right). \tag{12}$$

The potential difference V between probes is then

$$V = V_{f_2} - V_{f_3} = \frac{\rho I}{2\pi}\left(\frac{1}{s_1} + \frac{1}{s_3} - \frac{1}{s_2 + s_3} - \frac{1}{s_1 + s_2}\right) \tag{13}$$

and the resistivity ρ is computable as

$$\rho = \frac{V}{I}\frac{2\pi}{\left(\dfrac{1}{s_1} + \dfrac{1}{s_3} - \dfrac{1}{s_1 + s_2} - \dfrac{1}{s_2 + s_3}\right)}. \tag{14}$$

When the point spacing is equal, that is $s_1 = s_2 = s_3 = s$, the above simplifies to

$$\rho = \frac{V}{I} 2\pi s. \tag{15}$$

[6] L. B. Valdes, "Effect of electrode spacing on the equivalent base resistance of point-contact transistors," PROC. I.R.E., vol. 40, pp. 1429–1434, eq. (26); November, 1952.

Case 2. Resistivity Probes Perpendicular to a Nonconducting Boundary

Consider as a boundary condition that the reflecting (nonconducting) boundary is a plane perpendicular to the plane which describes the surface of the material on which the resistivity measurements are done. For this case the line on which the resistivity probes lie is assumed to be perpendicular to the line which corresponds to the intersection of the planes of the top surface and the boundary.

The relation between measured voltage and current in the four point probes and the resistivity of the material can be obtained from the model of Fig. 3. Images of the current sources are used and the floating potential at the potential probes is calculated as before. If the boundary is reflecting (nonconducting) the images are current sources of the same sign. Equal spacing between probes is assumed for simplicity.

The floating potential V_{f_2} at probe (2) is given by

$$V_{f_2} = \frac{\rho I}{2\pi}\left(\frac{1}{s} - \frac{1}{2s} - \frac{1}{2l+2s} + \frac{1}{2l+5s}\right). \quad (16)$$

Similarly the floating potential V_{f_3} at probe (3) can be obtained and the difference is

$$V = \frac{\rho I}{2\pi s}\left(1 + \frac{s}{2l+s} - \frac{s}{2l+2s} - \frac{s}{2l+4s} + \frac{s}{2l+5s}\right). \quad (17)$$

The resistivity then is

$$\rho = \frac{V}{I}\, 2\pi s\, \frac{1}{\left(1 + \dfrac{s}{2l+s} - \dfrac{s}{2l+2s} - \dfrac{s}{2l+4s} + \dfrac{s}{2l+5s}\right)} \quad (18)$$

or

$$\rho = \rho_0 F_2\left(\frac{l}{s}\right) \quad (19)$$

where ρ_0 is the resistivity computed from (15) and $F_2(l/s)$ is the function plotted in Fig. 4.

TABLE I

l/s	$F_2(l/s)$	$F_3(l/s)$	$F_4(l/s)$	$F_5(l/s)$
0	0.69	0.5	1.82	∞
0.2	0.79	0.533	1.365	8.07
0.5	0.882	0.658	1.182	2.08
1.0	0.947	0.842	1.060	1.232
2.0	0.992	0.965	1.010	1.038
5.0	0.996	0.997	1.004	1.003
10.0	0.9995	0.9996	0.0005	1.0004

The resistivity ρ_0 may be obtained from (14) when the probe spacings s_1, s_2, and s_3 are approximately equal. Table I shows the values of $F_2(l/s)$ used for plotting Fig. 4. The function was calculated from

$$F_2\left(\frac{l}{s}\right) = \frac{1}{1 + \dfrac{1}{1+2l/s} - \dfrac{1}{2+2l/s} - \dfrac{1}{4+2l/s} + \dfrac{1}{5+2l/s}}. \quad (20)$$

Case 3. Resistivity Probes Parallel to a Nonconducting Boundary

The boundary of the surface on which the measurements are made is assumed to lie on a nonconducting plane perpendicular to the surface. The four probes are assumed to lie in a line parallel to the intersection of the two planes.

The model for this case is in Fig. 5. As in the previous case, the images are current sources of the same sign since the boundary is reflecting or nonconducting. The floating potentials V_{f_2} and V_{f_3} at probes (2) and (3) are identical in form so that the difference is

$$V = V_{f_2} - V_{f_3} = 2V_{f_2} \quad (21)$$

and

$$\rho = \frac{V}{I}\, 2\pi s\, \frac{1}{2\left(\dfrac{1}{2} + \dfrac{s}{\sqrt{s^2 + (2l)^2}} - \dfrac{s}{\sqrt{(2s)^2 + (2l)^2}}\right)} \quad (22)$$

or

$$\rho = \rho_0 F_3\left(\frac{l}{s}\right). \quad (23)$$

The resistivity ρ_0 can be computed from (14) or (15) and

$$F_3\left(\frac{l}{s}\right) = \frac{1}{\left[1 + \dfrac{2}{\sqrt{1+\left(\dfrac{2l}{s}\right)^2}} - \dfrac{1}{\sqrt{1+\left(\dfrac{l}{s}\right)^2}}\right]}. \quad (24)$$

This function is tabulated in Table I and plotted in Fig. 6.

Case 4. Resistivity Probes Perpendicular to a Conducting Boundary

The same geometry as in Case 2 is assumed here, except that the boundary is conducting and the sign of the images has to be reversed. Fig. 3 serves as a model, except that image (5) is positive and image (6) is negative. Then

$$\rho = \frac{V}{I}\, 2\pi s\, \frac{1}{\left(1 - \dfrac{s}{2l+s} + \dfrac{s}{2l+2s} + \dfrac{s}{2l+4s} - \dfrac{s}{2l+5s}\right)} \quad (25)$$

and

$$F_4\left(\frac{l}{s}\right) = \frac{1}{1 - \dfrac{1}{1+\dfrac{2l}{s}} + \dfrac{1}{2+\dfrac{2l}{s}} + \dfrac{1}{4+\dfrac{2l}{s}} - \dfrac{1}{5+\dfrac{2l}{s}}}. \quad (26)$$

The function $F_4(l/s)$ is tabulated in Table I and plotted in Fig. 7.

Case 5. Resistivity Probes Parallel to a Conducting Boundary

The same geometry as in Case 3 is assumed here, except that the boundary is conducting and the sign of the images must be reversed. Therefore, Fig. 5 is the model with image (5) negative and image (6) positive. From this

$$\rho = \frac{V}{I} \, 2\pi s \, \frac{1}{2\left(\dfrac{1}{2} - \dfrac{s}{\sqrt{s^2 + (2l)^2}} + \dfrac{s}{\sqrt{(2s)^2 + (2l)^2}}\right)} . \quad (27)$$

The function

$$F_5\left(\frac{l}{s}\right) = \frac{1}{\left[1 - \dfrac{2}{\sqrt{1 + \left(\dfrac{2l}{s}\right)^2}} + \dfrac{1}{\sqrt{1 + \left(\dfrac{l}{s}\right)^2}}\right]} \quad (28)$$

is tabulated in Table I and plotted in Fig. 8.

Case 6. Resistivity Measurements on a Thin Slice-Conducting Bottom Surface

Two boundary conditions must be met on this case; the top surface of the slice must be a reflecting (nonconducting) surface and the bottom surface must be an absorbing (conducting) surface. Since the two boundaries are parallel a solution by the method of images requires for each current source an infinite series of images along a line normal to the planes and passing through the current source.
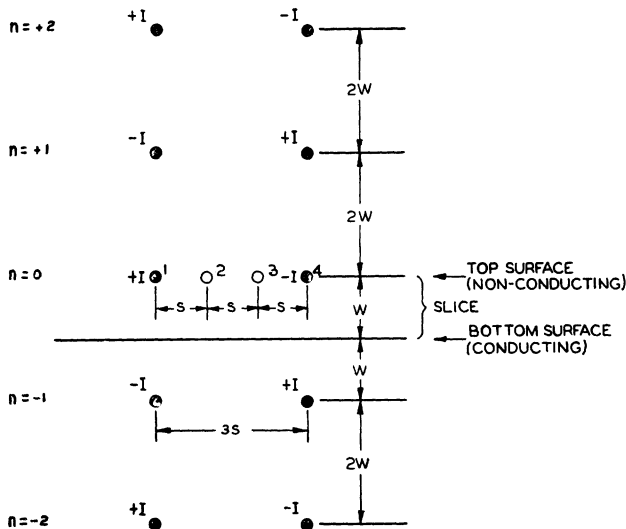

Fig. 15—Images for the case of the resistivity probes on a thin slice with a conducting bottom surface.

The model for this case is shown in Fig. 9. The side surfaces of the die are assumed to be far from the area of measurement and, therefore, only the effect of the bottom surface needs to be considered. In this analysis

equal probe spacing s shall be assumed. The width of the slice is w. The array of images needed is indicated in Fig. 15, where the polarity and spacings of the first few images are as shown.

The floating potential V_{f_2} at electrode (2) is:

$$V_{f_2} = \frac{\rho I}{2\pi}\left[\sum_{n=-\infty}^{n=\infty}(-1)^n\frac{1}{\sqrt{s^2 + (2nw)^2}} - \sum_{n=-\infty}^{n=\infty}(-1)^n\frac{1}{\sqrt{(2s)^2 + (2nw)^2}}\right]. \quad (29)$$

Likewise, the floating potential at electrode (3) can be obtained and

$$V = \frac{\rho I}{2\pi}\left[\frac{1}{s} + \sum_{n=1}^{n=\infty}(-1)^n\frac{4}{\sqrt{s^2 + (2nw)^2}} - \sum_{n=1}^{n=\infty}(-1)^n\frac{4}{\sqrt{(2s)^2 + (2nw)^2}}\right]. \quad (30)$$

The resistivity then becomes

$$\rho = \frac{\rho_0}{G_6\left(\dfrac{w}{s}\right)} . \quad (31)$$

Where resistivity ρ_0 is computable from (15), and (14) can be used if the point spacings are different, but approximately equal. The function $G_6(w/s)$ is computed from[7]

$$G_6\left(\frac{w}{s}\right) = 1 + 4\,\frac{s}{w}\sum_{n=1}^{n=\infty}(-1)^n\left\{\frac{1}{\sqrt{\left(\dfrac{s}{w}\right)^2 + (2n)^2}} - \frac{1}{\sqrt{\left(2\,\dfrac{s}{w}\right)^2 + (2n)^2}}\right\}, \quad (32)$$

which is tabulated in Table II and plotted in Fig. 10.

TABLE II

W/S	$G_6(W/S)$	$G_7(W/S)$
0.100	0.0000019	13.863
0.141	0.00018	9.704
0.200	0.00342	6.931
0.333	0.0604	4.159
0.500	0.228	2.780
1.000	0.683	1.504
1.414	0.848	1.223
2.000	0.933	1.094
3.333	0.983	1.0228
5.000	0.9948	1.0070
10.000	0.9993	1.00045

[7] A neat way of summing the series has been suggested by A. Uhlir, to be published.

Case 7. Resistivity Measurements on a Thin Slice-Non-conducting Bottom Surface

The model for these measurements is like for Case 6, except that the bottom surface of the slice is nonconducting. This means that all the images of Fig. 15 have the same charge as the current source. Thus all the images on a row have equal charges and (30) describes the potential difference across the inner pair of probes if $(-1)^n$ is removed from the equation. Then,

$$\rho = \frac{\rho_0}{G_7\left(\dfrac{w}{s}\right)} \qquad (33)$$

where

$$G_7\left(\frac{w}{s}\right) = 1 + 4\,\frac{s}{w}\sum_{n=1}^{n=\infty}\left[\frac{1}{\sqrt{\left(\dfrac{s}{w}\right)^2 + (2n)^2}}\right.$$

$$\left. - \frac{1}{\sqrt{\left(2\,\dfrac{s}{w}\right)^2 + (2n)^2}}\right]. \qquad (34)$$

This function $G_7(w/s)$ is tabulated in Table II and plotted in Fig. 11. For smaller values of w/s the function $G_7(w/s)$ approaches the case for an infinitely thin slice, or

$$G_7\left(\frac{w}{s}\right) = \frac{2s}{w}\ln 2. \qquad (35)$$

Acknowledgment

This paper presents the curves needed to compute resistivity under a large number of different experimental conditions. The accuracy of the results is better than 2 per cent in practically all cases. The assistance of F. R. Keene, who carried out most of the computations of tables and who obtained the experimental results, is gratefully acknowledged. The author is also indebted to A. Uhlir, W. J. Pietenpol, and R. M. Ryder.

A General RLC Synthesis Procedure*

LOUIS WEINBERG†

Summary—Any physically realizable RLC transfer function—impedance, admittance, or dimensionless ratio—can be realized within a multiplicative constant by the synthesis procedures presented in this paper. The form of network achieved is a lattice with these significant features: (a) it may have any desirable termination; (b) it contains no mutual inductance; (c) every inductance in the network appears with an associated series resistance so that, in building the network, low-Q coils may be used.

In addition, the lattice arms are of so simple a form relative to each other that many of the achieved lattices are amenable to reduction to unbalanced networks. Further, in case of a transfer admittance, reduction can be achieved with the use at most of real transformers i.e., transformers with winding resistance, finite magnetizing inductance, and a coupling coefficient smaller than one.

I. Introduction

THERE IS A wide variety of existing synthesis procedures, but as anyone conversant with the synthesis field fully realizes much remains to be done. The inadequacy of available procedures shows up particularly in a broad field of communications, namely, synthesis for prescribed transient response.[1] In this synthesis both magnitude and phase are important, so that the methods for realizing a prescribed magnitude of transfer function are inapplicable. Up to the present time one of the principal procedures that could be used for the realization of both minimum-phase and non-minimum-phase transfer functions has been the one that yields a constant-resistance lattice. This type of lattice suffers from many disadvantages. In general each of the

[1] D. F. Tuttle, Jr.: "Network Synthesis for Prescribed Transient Response," Sc.D. thesis in electrical engineering, M.I.T., Cambridge, Mass.; 1948.